La Metallurgia Italiana
International Journal of the Italian Association for Metallurgy

Kinetics of strain aging in grade 1.4003 ferritic stainless steel

T. Manninen, P. Peura

Static strain aging of grade 1.4003 ferritic stainless steel was investigated. The test material was pre-strained to 5% elongation under uniaxial tension and subsequently aged at temperatures between 200°C and 300°C. The aging time was varied between one hour and one week. The kinetics of strain aging were evaluated based on increments in the yield strength produced by the heat treatments. The aging heat treatment caused the reappearance of a clearly defined yield point in all cases. The obtained strength increments were between 30 and 60 MPa. The apparent activation energy of the process was 128 kJ/mol. The obtained activation energy agrees with the literature values for interstitial diffusion in high-chromium Fe-Cr alloys determined with internal friction measurements.

KEYWORDS: FERRITIC STAINLESS STEEL, EN 1.4003, KINETICS, STATIC STRAIN AGING

INTRODUCTION

Bake-hardening steels are commonly used to manufacture automotive exterior body parts such as roofs, hoods, and door outer panels, i.e., parts that are painted after forming into shape. These steels are designed to achieve a significant increase in yield strength during the low-temperature heat treatment performed to cure the paint. The gain in yield strength produced by the paint baking can range from 30 MPa to 50 MPa. The increased final strength provides improved dent resistance for the car body. Bake-hardening utilizes the phenomenon of strain aging. Strain aging is common in metals having a body-centered cubic structure. The kinetics of the process are controlled by the long-range diffusion of interstitials to the stress field surrounding dislocations. Therefore, the required aging time and temperature depend on the diffusivity of interstitials in the metal. [1]

The grade 1.4003 is unstabilized 12% chromium ferritic stainless steel designed for structural applications. In contrast to many other ferritic stainless steel grades, 1.4003 has the weldability and toughness properties required of structural applications at sub-zero conditions. Grade 1.4003 is often used as cold-formed tubes and profiles to construct lightweight bus body frames. An increased in-service dent and impact resistance would be advantageous in this application.

Since the classical theory of strain aging was developed in the 1940s by Cottrell and Bilby [2], numerous studies

Timo Manninen
Outokumpu Research and Development, Tornio, Finland

Pasi Peura
Tampere University, Tampere, Finland

have been made on static strain aging of low-carbon steel. In contrast, the research on static strain aging in ferritic stainless steels is limited. Buono et al. [3] studied the kinetics of strain aging in unstabilized 16% Cr grade 1.4016 in solution annealed state. The specimens were pre-strained in uniaxial tension to a uniform elongation of 5% and heat treated at temperatures between 80°C and 200°C; the aging time varied between 10 minutes and 2 hours. A significant bake-hardening effect was observed. The activation energy of aging was determined to be 127 kJ/mol. This value is significantly higher than the activation energy of about 80 kJ/mol for ultralow carbon bake hardening steels. The value 80 kJ/mol corresponds to the activation energy of diffusion of interstitial C and N atoms in pure α-iron. Kaçar et al. [4] studied the bake-hardening of grade 1.4016 both in as-received and solution-annealed condition. The test materials were pre-strained 5 % in uniaxial tension and aged between 100°C and 400°C for 30 minutes. A significant increase in the yield and tensile strength was obtained. The strength of the solution-annealed test material was higher than that of the as-received test material at all aging temperatures. Palosaari et al. [5] investigated bake hardening of 18% Cr stabilized grades 1.4509 and 1.4521 in as-received condition. They showed that stabilized ferritic stainless steel grades are also susceptible to strain aging despite having abundant stabilizing elements to entrap interstitials. The maximum increment of yield strength caused by the bake-hardening was approximately 50 MPa. The activation energies were 151 kJ/mol and 146 kJ/mol. The activation energies were again considerably higher than those reported for low-carbon bake-hardening steels. The bake hardening of low chromium ferritic stainless grade 1.4003 was recently studied by Fu et al. [6,7]. Fu determined the bake-hardening index values for this grade in as-received condition. The test material was pre-strained to 2%, 6%, or 10% tensile elongation and subsequently aged at 170°C or 210°C for 20 minutes. The increment in the yield strength produced by the aging heat treatment ranged from 15 MPa to 33 MPa. The results showed that static strain aging can increase the yield strength of low chromium unstabilized ferritic stainless steel 1.4003. The study concentrated mainly on paint baking times. The full extent of the hardening response was most likely not achieved due to low aging temperature and short aging time. Furthermore, the results obtained in this study do not provide any information regarding the kinetics of the aging process.

The existing literature data does not provide any information on the kinetics of static strain aging of commercial grade 1.4003 ferritic stainless steel in the as-received state. Therefore, this research aimed to characterize the kinetics of strain aging of this steel grade in the as-received condition. Knowledge of the kinetics of the aging process is needed to determine the full extent of the hardening response and optimize the possible heat treatments for improving the material performance.

MATERIAL

The test material was commercial grade EN 1.4003 ferritic stainless steel with a thickness of 4mm and a surface finish of 2E. The chemical composition of the test material is given in Table 1. The microstructure of the test material was characterized with optical microscopy and electron backscatter diffraction (EBSD). The EBSD measurements were made using a Leo 1450VP scanning electron microscope equipped with an HKL NordlysF detector and HKL Fast Acquisition software. The step size was 0.1 μm. The microstructure was characterized as fine-grained ferrite with large chromium carbides. No retained austenite or martensite was observed. The grain size number of ferrite, measured according to ASTM E112, was G = 11.8. This value corresponds to the average grain diameter of 6 μm.

The mechanical properties of the test material measured in the transverse direction are summarized in Table 2. The test material was produced ten years ago. Still, the Rp0.2 and Rm values measured in the present study were within ±3 MPa of the values in the material certificate issued ten years ago. Therefore, our tensile test results confirm that ferritic stainless steel does not age at room temperature, as discussed by Alvarez de Sotomayor et al. [8].

Tab.1 - The chemical composition of the test material (wt-%).

Chemical composition							
C	Si	Mn	P	S	Cr	Ni	N
0.007	0.26	1.41	0.028	0.001	11.3	0.4	0.016

Tab.2 - The mechanical properties of the test material measured according to EN ISO 6892-1 method A223.

Tensile test results						
Rp0.1 (MPa)	Rp0.2 (MPa)	Rp1.0 (MPa)	Rp5.0 (MPa)	Rm (MPa)	Ag (%)	A50 (%)
388	393	406	478	525	17.0	28.3

METHODS

The testing procedure consisted of four distinct stages. First, standard tensile testing specimens were machined from the test material parallel to the transverse direction. Then, each specimen was prestrained to a 5.0% permanent elongation using a tensile testing machine; the loading rate was 0.00025 1/s. The prestrained specimens were aged at 200°C, 250°C, or 300°C in a laboratory furnace; the soaking time varied between 30 minutes and one week. The heat treatment was followed by air cooling to ambient temperature. During the heat treatments and subsequent cooling, the temperature of each specimen was measured with a K-type thermocouple. The effective soaking time t_s was computed based on the temperature T during heating, soaking, and cooling as follows:

$$t_s = \frac{1}{T_s} \int_0^{t_{end}} T(x)\ dx \tag{1}$$

where T is the specimen temperature, T_s is the soaking temperature, and t_{end} is the time needed for the specimen to cool back to room temperature after the heat treatment. The effective soaking time was approximately 30 minutes longer than the nominal one.

The tensile properties of aged specimens were measured according to EN ISO 6892-1 method A223. The tensile properties of aged specimens were compared with those of un-aged, prestrained specimens. The strain aging response was quantified by the changes in the stress-strain response defined in Fig. 1.

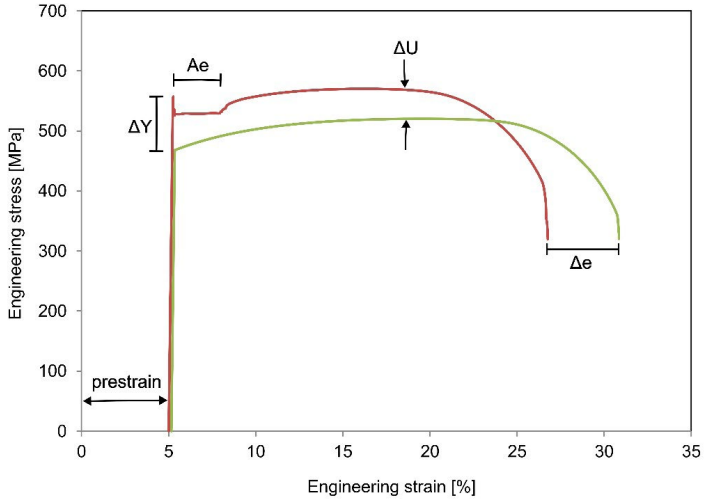

Fig. 1 - Definition of entities ΔY, Ae, ΔU, and Δe used as measures for the strain aging response. The green line shows the response of the prestrained specimen, and the red line shows the response of the prestrained and aged specimen.

RESULTS

The aging heat treatment restored the pronounced yield point at all aging temperatures; the prestrained, unaged specimens showed continuous yielding. As shown in Figs. 2 and 3, the yield strength ΔY and yield point elongation A_e increased with aging temperature and time. It may also be seen that the increment in the yield stress did not increase after 48.5 hours of aging at T = 300°C. Therefore, it was concluded the aging process was very close to completion in the two most prolonged heat treatments. Hence, the saturation value for the increment in the yield stress produced by the aging process was estimated as 57 MPa.

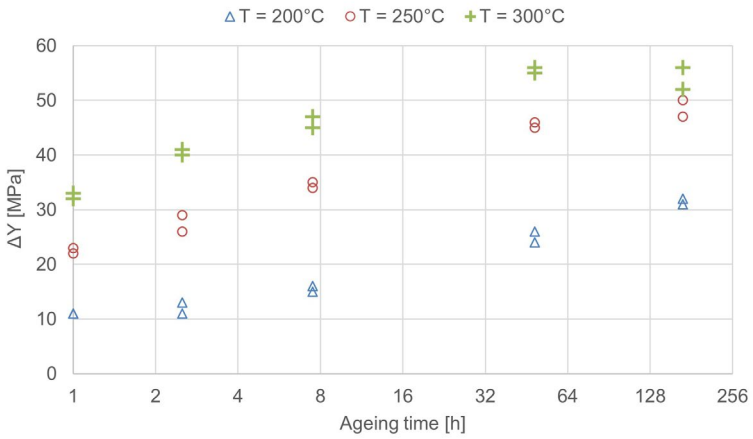

Fig. 2 - The increment of yield strength, ΔY, caused by isothermal aging.

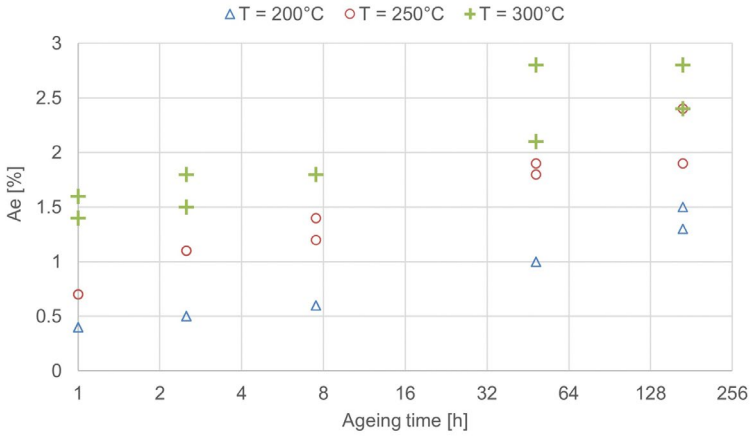

Fig. 3 - The yield point elongation, Ae, increases with increasing aging temperature and time.

Following Buono et al. [3], the aging kinetics was modeled with the Johnson–Mehl–Avrami–Kolmogorov (JMAK) equation

$$W = 1 - \exp[-(kt)^n] \tag{2}$$

where W is the aged volume fraction, and t is the aging time. Assuming that the increase in the yield strength is caused by the strain aging, the volume fraction of aged material can be estimated with

$$W = \frac{\Delta Y}{\Delta Y_{max}} \tag{3}$$

where ΔY_{max}=57 MPa is the saturation value for ΔY. Aging is a thermally activated process. Consequently, the rate coefficient k can be modeled with the Arrhenius equation

$$k(T) = k_0 \exp\left[-\frac{Q}{RT}\right] \quad (4)$$

where k_0 is an unknown material parameter, Q is the activation energy of the aging process, R is the universal gas constant, and T is the absolute temperature. The equation can be written as

$$\ln \ln\left(\frac{1}{1-W}\right) = n \ln k(T) + n \ln t \quad (5)$$

Fig. 4 shows the entity ln $\ln(1/(1\text{-}W))$ as a function of ln t. Since the measurements obtained at three different temperatures form straight lines with the same slope, the aging kinetics follows Eq. (2). The slope of the lines provides the value n = 0.29 for the time exponent.

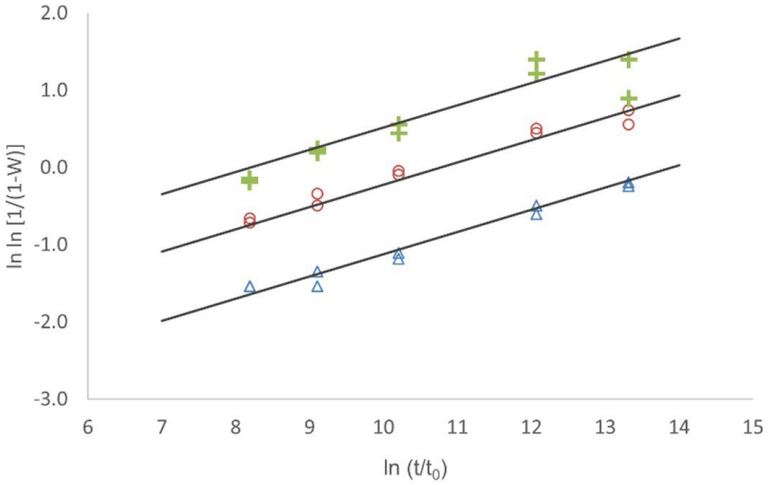

Fig. 4 - The measurement data form three straight lines with the same slope when plotted in transformed coordinates. The parameter t_0 equals one second.

The pre-exponential factor k_0 and the activation energy Q were determined using multilinear regression analysis based on Eqs. 4 and 5. The values of the model parameters are summarized in Tab. 3. Figs. 5 and 6 show that an excellent correspondence was obtained between the measured values and model prediction. The standard error of the model was S = 1.8 MPa.

Tab.3 - The determined model parameters.

Kinetic model parameters		
k_0	Q	n
$1.3 \cdot 10^8$ 1/s	128 kJ/mol	0.29

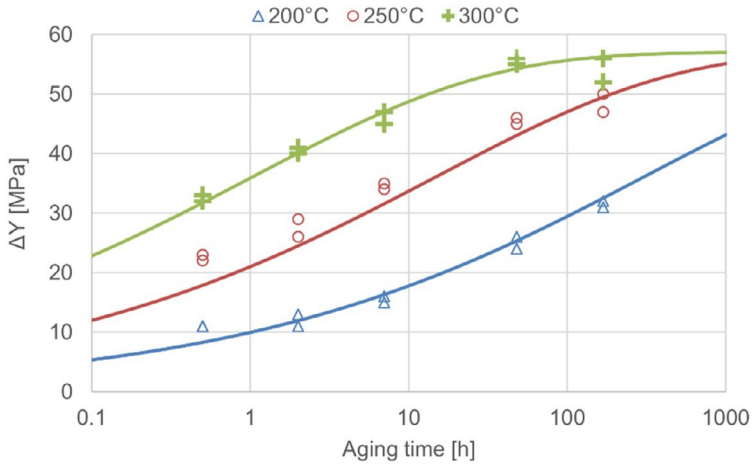

Fig. 5 - Measured and predicted increment in the yield strength.

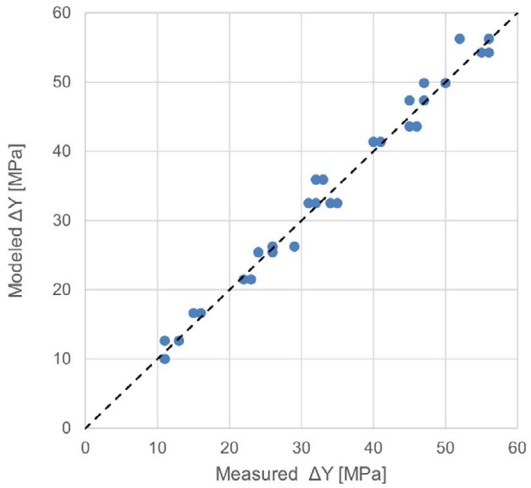

Fig. 6 - Correspondence between measure and predicted increment in the yield strength.

DISCUSSION

Table 4 shows a comparison of kinetic parameters obtained in the present work and published values for ferritic steel grades. The values Harper [9] has reported for pure α-iron are also shown for reference. It may be seen that the activation energy obtained in the present work is in good agreement with those reported elsewhere for ferritic stainless steel grades. Golovin et al. [10] determined the activation energy for diffusion of carbon in high-chromium ferritic steels using internal friction experiments. The test materials contained 8 to 35 weight percentages chromium. The obtained activation energy values increased with increasing chromium content and ranged from 119 kJ/mol to 141 kJ/mol for the 8% and 35% chromium alloys. A parabolic fit to the activation energy values given by Golovin et al. suggests that the activation energy for the diffusion of carbon in Fe-Cr alloys containing 11.5% and 16.5% chromium would be Q = 122 kJ/mol and Q = 129 kJ/mol, respectively. These values are in excellent agreement with activation energies determined in the present work for 11.5% Cr and that determined by Buono et al. [3] for 16.5% Cr ferritic stainless steels.

The activation energies in Table 4 are significantly higher for ferritic stainless steel grades than for α-iron. Golovin et al. [10] argued that chromium atoms produce nonequivalent interstitial positions, thereby increasing the activation energy. This hypothesis was recently questioned by Herschberg et al. [11], who modeled the internal friction and tracer diffusion experiments in ideal Fe-Cr-C alloys using atomistic methods. They used density functional theory (DFT) to calculate the bond energy and energy of migration for carbon atoms. The

calculated values were used to simulate internal friction and tracer diffusion experiments in Fe-Cr-C alloys with 0% and 100% chromium. Their results did not agree with the experimental study of Golovin et al.; the increase in the activation energy for the diffusion of carbon was significantly smaller than that observed by Golovin et al. Therefore, Herschberg et al. suggested that the notable increase in the activation energy observed in the earlier study was produced by the interaction of carbon with defects such as dislocations and vacancies.

An alternative explanation might be proposed based on the work of Čermák and Král [12]. They studied the diffusion in carbon-supersaturated ferrite. The test materials included pure α-iron and Fe-Cr binary alloy with 15% chromium. In both cases, the diffusion of carbon could be described with the Arrhenius equation. Carbon diffusion was independent of chromium's presence in the matrix; the activation energy for the diffusion of carbon was 158 kJ/mol in both model materials. It was concluded that the carbon atoms diffuse in ordered structures rather than individual atoms in the supersaturated matrix. This conclusion is supported by Kabir et al. [13], who studied the diffusion in the Fe-C system using density functional theory. They concluded that complexes containing one vacancy and two carbon atoms are abundant in carbon-rich ferrite. These complexes are immobile. The calculated binding energy of this vacancy cluster was 1.46 eV, i.e., 0.73 eV/atom (70 kJ/mol). The activation energy associated with the transference of carbon atoms from the cluster to the locations around dislocations should be equal to the sum of the binding energy of the cluster molecule and the activation energy for the diffusion of carbon atoms, i.e., 154 kJ/mol. This value agrees with the activation energy obtained by Čermák and Král [12] for supersaturated ferrite.

The activation energy for aging in different ferritic stainless steel grades is, without exception, significantly higher than the values reported for α-iron. The presence of chromium atoms does not considerably increase the activation energy of carbon diffusion in ferrite [11,12], whereas the carbon diffusion is slowed down in the carbon-supersaturated ferrite [12]. Therefore, the most likely reason for the higher activation energy in ferritic stainless steels is that the ferrite is supersaturated with carbon at aging temperatures. In pure α-iron, ferrite is in equilibrium with cementite (Fe_3C), whereas in ferritic stainless steel, the equilibrium carbide is $Cr_{23}C_6$. Cementite precipitation is expected to be considerably faster than chromium carbide since the former does not require diffusion of substitutional Cr atoms. The activation energy for bulk diffusion of chromium in ferrite is high, 250 kJ/mol [14]. Therefore, the precipitation of cementite will be faster than that of the chromium carbide when the steel strip is cooled after final annealing in a continuous annealing line. It is also possible that the chromium alloying reduces the solubility of carbon in ferrite. In this case, a considerably smaller concentration of carbon atoms will produce a supersaturated ferrite.

In the original theory for static strain aging in low-carbon steels by Cottrell and Bilby [2], the time exponent equals n = 2/3. As discussed by Lement and Cohen [15], this particular value is related to the assumption that the depletion of carbon atoms occurs in a cylindrical volume surrounding randomly situated dislocation lines. By assuming that the dislocations are arranged in cell walls, as they usually are in ferritic stainless steels and other metals with high stacking-fault energy, the geometry of carbon flow is changed from two-dimensional to one-dimensional and the time exponent is reduced to n = 1/3. The time exponent obtained in the present study, n = 0.29, is close to Lement and Cohen's theoretical value.

The obtained strength increments of 30-60 MPa are comparable to those of bake-hardenable low-carbon steels used in the automotive industry [1]. The increment in the yield strength was, however, relatively modest compared to the relatively high yield strength of the cold-worked material. Furthermore, a long soaking time at a relatively high temperature was needed to achieve the highest improvements in the mechanical properties. Therefore, it seems likely that the processing costs may be high compared to the strength increment produced.

Tab.4 - Comparison of activation energy and time exponent values.

Kinetic model parameters			
Material	Q	n	Ref.
Unstabilized 11.5% Cr ferritic stainless steel 1.4003	$128\,\frac{kJ}{mol}$	0.29	This work
Unstabilized 16.5% Cr ferritic stainless steel 1.4016	$127\,\frac{kJ}{mol}$	0.36 – 0.47	[3]
Stabilized 18% Cr ferritic stainless steels 1.4509	$151\,\frac{kJ}{mol}$	0.19 – 0.24	[5]
Stabilized 18% Cr ferritic stainless steels 1.4521	$146\,\frac{kJ}{mol}$	0.16 – 0.30	[5]
α-iron	$84\,\frac{kJ}{mol}$	2/3	[9]

SUMMARY AND CONCLUSIONS

Our results show that low chromium ferritic stainless steel grade 1.4003 is susceptible to strain aging. The aging heat treatment restored the pronounced yield point at all aging temperatures. Furthermore, the yield strength and yield point extension increased with increasing aging temperature and time. The apparent activation energy of the process was 128 kJ/mol. While this value is considerably higher than the typical value of about 80 kJ/mol for α-iron and for bake hardenable low-carbon steels, it agrees with the literature value for interstitial diffusion in high-chromium Fe-Cr alloys determined with internal friction measurements. The strength increments are comparable to bake-hardenable low-carbon steels used in the automotive industry. The increments were, however, relatively modest compared to the relatively high yield strength of the cold-worked material. Furthermore, a long soaking time at a relatively high temperature was needed to achieve the highest improvements in the mechanical properties. Therefore, the processing costs may be too high compared to the modest strength increment produced.

REFERENCES

[1] Baker L, Daniel S, Parker J. Metallurgy and processing of ultralow carbon bake hardening steels. Materials Science and Technology. 2002;18:355–368.
[2] Cottrell AH, Bilby BA. Dislocation theory of yielding and strain ageing of iron. Proceedings of the Physical Society Section A. 1949;62:49.
[3] Buono V, Gonzalez B, Andrade M. Strain aging of AISI 430 ferritic stainless steel. Scripta materialia. 1997;38:185–190.
[4] Kaçar R, Gündüz S. Increasing the strength of AISI 430 ferritic stainless steel by static strain ageing. Kovove Mater. 2009;47:185–191.
[5] Palosaari M, Manninen T. Bake-hardening of stabilized ferritic stainless steels. Special Edition of Steel Research International for Metal Forming 2012, Wiley-VCH Verlag GmbH. 2012;951–954. Available from https://onlinelibrary.wiley.com/page/journal/1869344x/homepage/metal-forming-2012.html
[6] Fu Z. A Study of Static Strain Aging of Selected Ferritic Steels. Master's thesis. Tampere University of Technology; 2017.
[7] Fu Z, Järvinen H, Manninen T, Peura P. Bake Hardening Behavior of 1.4003 Ferritic Stainless Steel. Ohutlevy. 2017;28–33.
[8] Alvarez de Sotomayor A, Herrera E. Permanent elimination of the yield-point phenomenon in AISI 430 stainless steel by skin-pass rolling. Journal of materials science. 1994;29:5833–5838.
[9] Harper S. Precipitation of carbon and nitrogen in cold-worked alpha-iron. Physical review. 1951;83:709.
[10] Golovin IS, Sarrak VI, Suvorova SO. Influence of carbon and nitrogen on solid solution decay. Metallurgical transactions A. 1992;23:2567–2579.
[11] Herschberg R, Fu C-C, Nastar M, et al. Atomistic modelling of the diffusion of C in FeCr alloys. Acta Materialia. 2019;165:638–653.
[12] Čermák J, Král L. Extremely slow carbon diffusion in carbon-supersaturated surface of ferrite. Kovove Mater. 2014;52:125–133.
[13] Kabir M, Lau TT, Lin X, et al. Effects of vacancy-solute clusters on diffusivity in metastable Fe-C alloys. Physical Review B. 2010;82:134112.
[14] Bowen AW, Leak GM. Solute diffusion in alpha-and gamma-iron. Metallurgical Transactions. 1970;1:1695–1700.
[15] Lement B, Cohen M. A dislocation-attraction model for the first stage of tempering. Acta Metallurgica. 1956;4:469–476.

TORNA ALL'INDICE >